Passive Dynamic Biped Catalogue, 1991

Tad McGeer
Vancouver, B.C., Canada
E-mail to USERTMCG@cc.sfu.ca

Symbols

(relevant formulae are referenced in parentheses)

Roman

c	axial position of mass centre (figure 12)
$\mathbf{C}$	matrix of control gains (22)
$\mathbf{I}$	identity matrix
g	gravitational acceleration
$\vec{H}$	angular momentum
l	leg length
m	mass
R	foot radius
r_{gyr}, r_g	radius of gyration
$\vec{S}$	stride function (1)
$\nabla\vec{S}$	jacobian of $\vec{S}$ (6)
$\nabla_1\vec{S}$	first row of $\nabla\vec{S}$ (23)
$\nabla_c\vec{S}$	gradient of $\vec{S}$ w.r.t. $\vec{u}$ (25)
$\nabla_T\vec{S}$	gradient of $\vec{S}$ w.r.t. T_H (20)
$\nabla_{T,1}\vec{S}$	first element of $\nabla_T\vec{S}$ (23)
T	torque
$\vec{u}$	vector of control variables (25)
V	translational velocity
w	forward offset from link axis to mass centre (Δy in figure 12)
w_{hip}	hip width (figure 12)
x	coordinate normal to the ground (figure 12)
y	coordinate along the slope (figure 12)
z	eigenvalue (7); lateral coordinate (figure 12)

Greek

α_0	leg pitch angle at support transfer
β	torso inclination
γ	slope, positive downhill
γ_g	slope for gravity-powered walking
Δy	forward offset from link axis to mass centre (figure 12)
Δz	lateral offset from link axis to mass centre (figure 12)
θ	pitch angle (figure 12)
$\vec{\nu}$	start-of-step state vector (1)
σ	dimensionless pendulum frequency (9)
τ	dimensionless time $t\sqrt{g/l}$
τ_0	step period
ϕ	roll angle (figure 12)
ψ	yaw angle (figure 12)
Ω	rotation rate in pitch
ω	rotation rate

Subscripts

0	steady cycle conditions
C	stance leg
F	swing leg
H	at the hip
k	step index
T	torso or hip

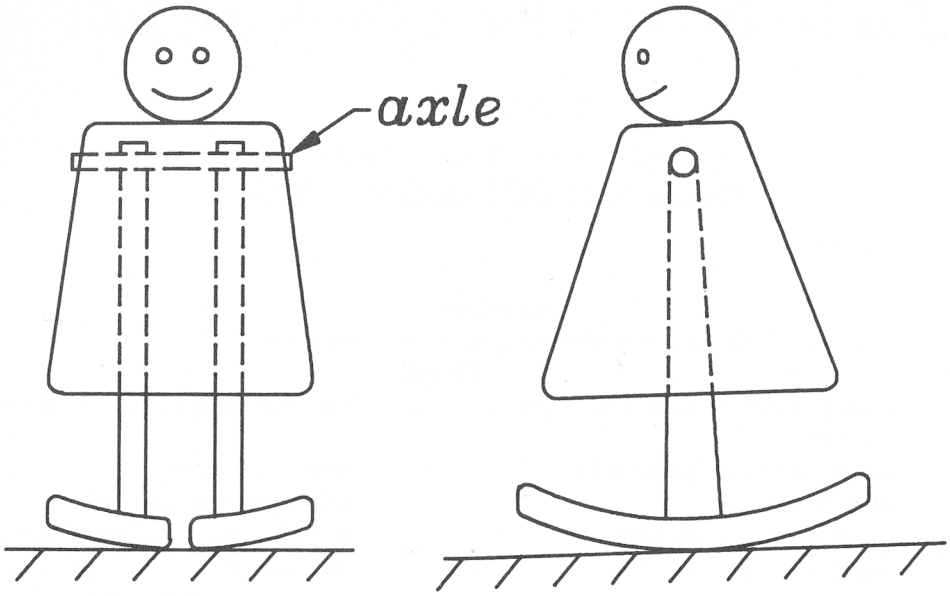

Figure 1: A bipedal toy which walks passively down shallow slopes. Energy gained by descending the slope is balanced by energy dissipated each time the swing foot hits the ground. The illustration is adapted from McMahon [8].

Abstract

Passive dynamic bipeds walk and run by virtue of physics inherent in the interaction of their legs and the ground; they need no motor control. A diverse spectrum of passive models are now known; together they offer a lively repertoire, including locomotion at various speeds, up and down hills, in two and three dimensions, and over unevenly-spaced footholds. We review the principal passive walkers investigated to date, including experimental results and references to detailed analyses. These suggest enticing opportunities for design of efficient and dextrous walking machines.

Perhaps legged locomotion has been imposed upon the roboticist's agenda by Hollywood. After all, as any moviegoer knows, *real* robots don't have wheels. Alternatively, perhaps the practical argument is genuinely compelling: legs do promise superb all-terrain transport, although one may be sceptical about applications in the near term. Or perhaps, as for me, their attraction is simply a conundrum. Wheels, wings, skates or skis obviously constitute a sound basis for travelling hither and yon: smooth, efficient, and devoid of any hint of complexity or needless appendage. But legs! All of those bits flailing around – hardly an obvious solution, and yet in their element so much more effective than any device on file in the patent office. To anyone guided by a faith in simplicity, the challenge is disconcerting. Can so successful a scheme be as contrived as it seems? If not, where is the simplicity?

The answer, I believe, lies in *passive dynamic walking.* Through this effect legged locomotion can proceed as a passive interaction of gravity and inertia, without any motor control. The effect is demonstrated most conclusively by the walking toy in figure 1, but our own steps are guided just as surely by the same simple physics. In fact dynamics

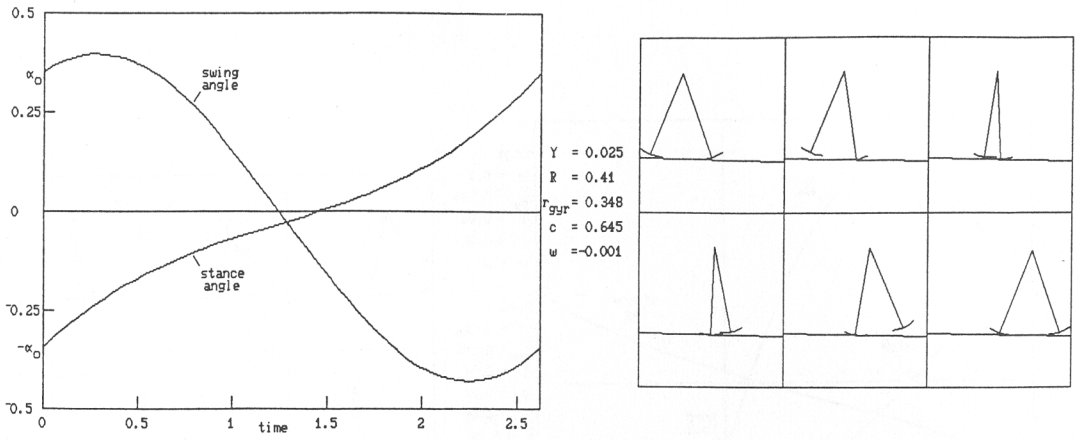

Figure 2: Passive dynamic walking cycle calculated for our first experimental biped descending a 2.5% slope. The plot shows stance and swing angles relative to the surface normal, as functions of time (made dimensionless by gravitational acceleration and leg length). The machine is modelled as two straight legs with semicircular feet and a pin joint at the hip. Parameters of the machine are tabulated in the margin.

of this sort can be seen in quite a variety of legged models, including devices having straight or knee-jointed legs (figures 2 and 3), with or without a torso (figure 4), moving in two dimensions or three (figure 5), and capable of walking or running (figure 6) or hopping (figure 7). Here we will concentrate on walking, tracing our own development from previously-reported work on simpler models through to newer results with knees and three-dimensional motion, and finally shining some light down paths for further experimental and analytical progress.

1 Straight-legged walking in 2D

Our experimental work on passive walking began with the machine shown in figure 8, which was essentially a two-dimensional version of the walking toy. We will not discuss it in detail, since a full report can be found elsewhere [3]. However a review is in order to indicate the central ideas in passive walking theory. The review begins at time zero in figure 2, when the step is just beginning and both legs are momentarily on the ground. The legs must at this instant be at equal and opposite angles ($\pm\alpha_0$), but their rotational speeds remain independently variable and so, at this instant, the model has three degrees of freedom: one angle plus two speeds. When this set is specified the subsequent motion is determined, and will proceed generally as shown in the figure. A small problem arises at midstride, when the swing foot attempts to drop below ground level (*cf.* figure 5) but contact can be prevented by briefly shortening the swing leg. Once the danger is past the leg can be reextended, and the motion then will continue until the legs again reach equal and opposite angles. At that point the forward foot hits the ground inelastically, dissipating some energy and changing the speeds of each leg The model is then poised to begin another step. If the speeds and angles at this instant are the same as they were at the beginning of the last step, then the model has hit upon a passively re-entrant cycle

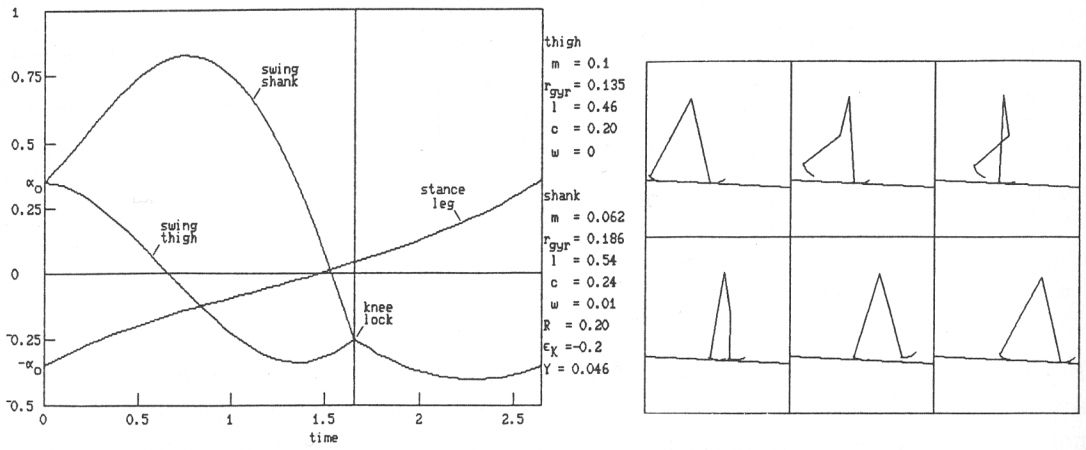

Figure 3: Passive cycle calculated for a pair of anthropomorphic legs having knees free in flexure but stopped against hyperextention. The slope is 4.6%. Model parameters are explained by McGeer [5].

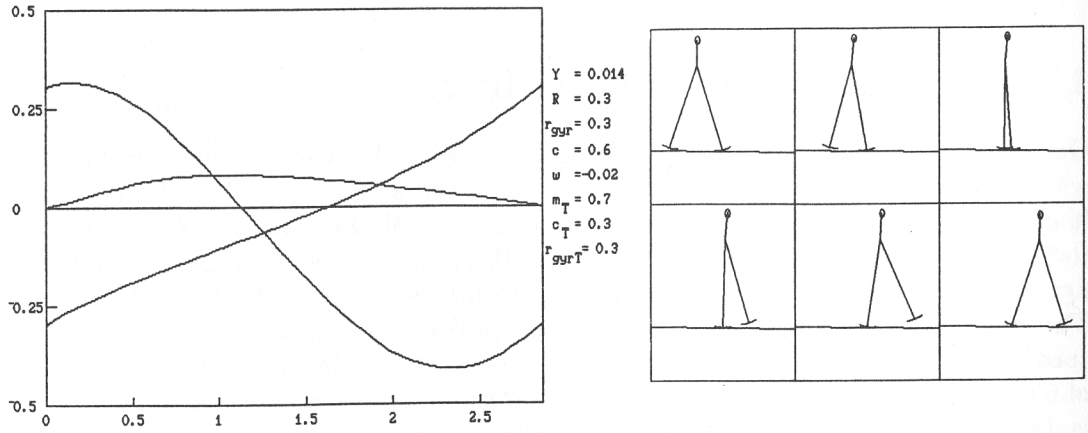

Figure 4: Walking cycle predicted for a straight-legged biped with a torso. This model leaves its legs free to swing passively, but holds its torso upright by actively controlling torque between the torso and stance leg [7].

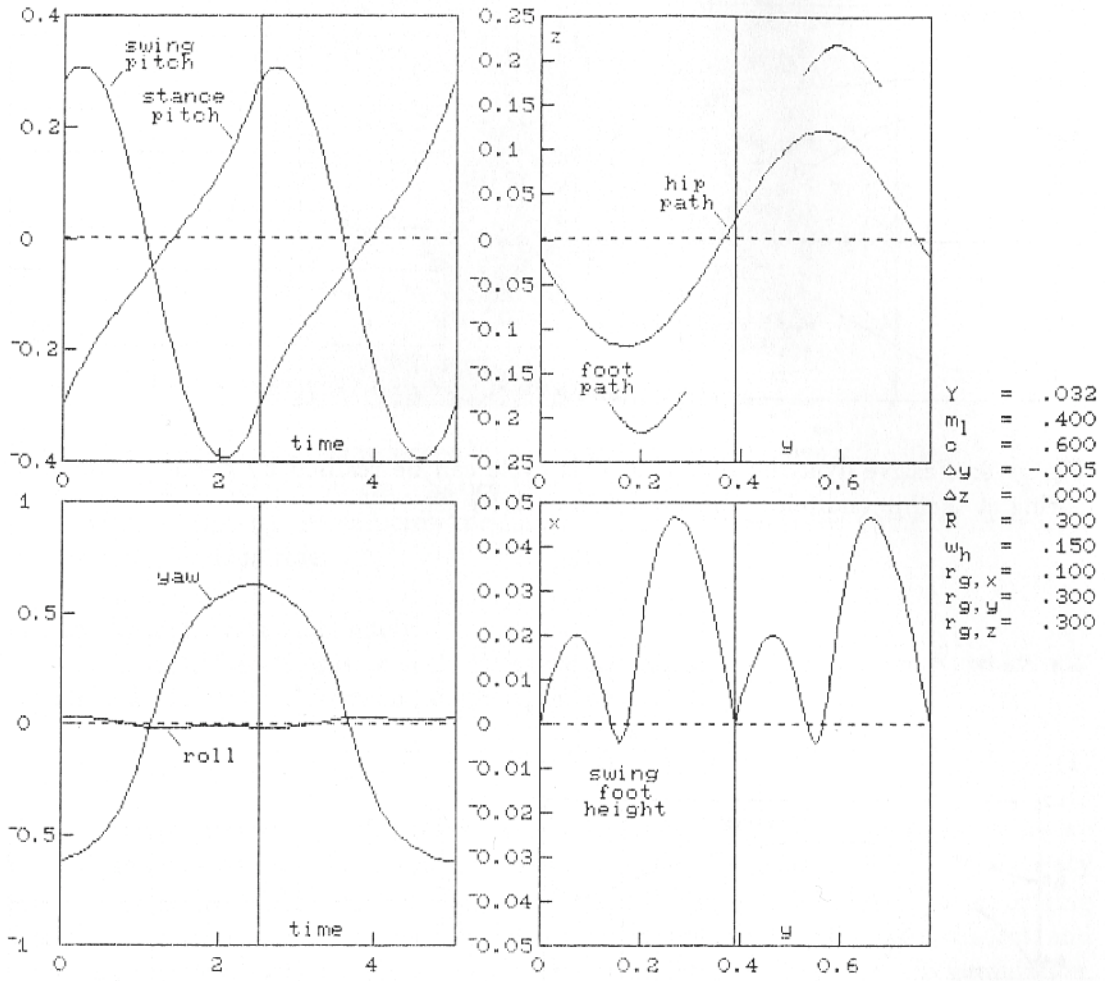

Figure 5: Three-dimensional passive cycle, as calculated for a straight-legged biped having legs separated by 15% of leg length. The slope is 3.2%. The legs' pitching motion is essentially the same as in two-dimensional passive walking, but to maintain lateral balance the model also develops a synchronised roll/yaw oscillation. In this example the yaw amplitude is substantially greater than the roll, and the cycle involves a pronounced lateral swaying of the hips (plotted in the upper right panel in units of leg length). As in the two-dimensional cycle the swing foot is calculated to pass slightly below ground level at midstride, but this problem could be remedied by knees.

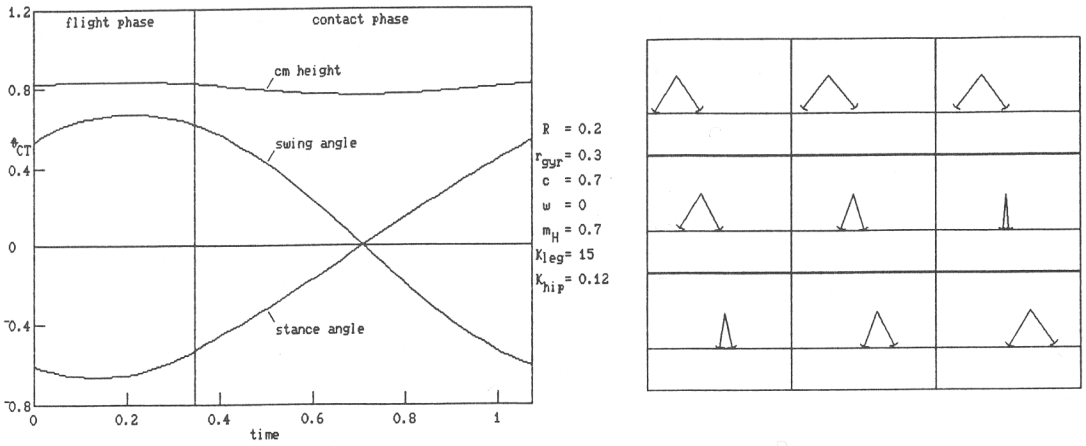

Figure 6: Passive dynamic running. This cycle can be realised by putting a torsional spring at the hip and telescopic springs in each leg [2].

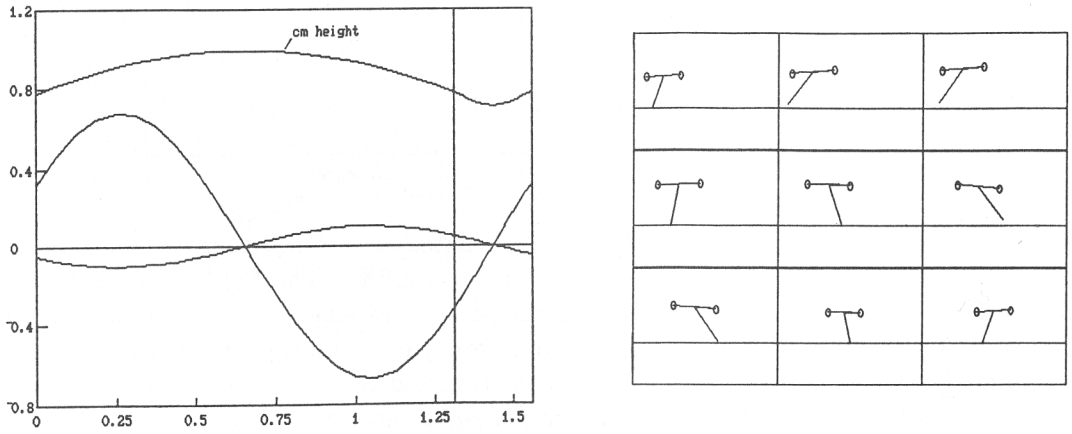

Figure 7: Passive dynamic hopping. Like passive running this cycle involves scissoring back and forth on a hip spring while bouncing on a leg spring [11].

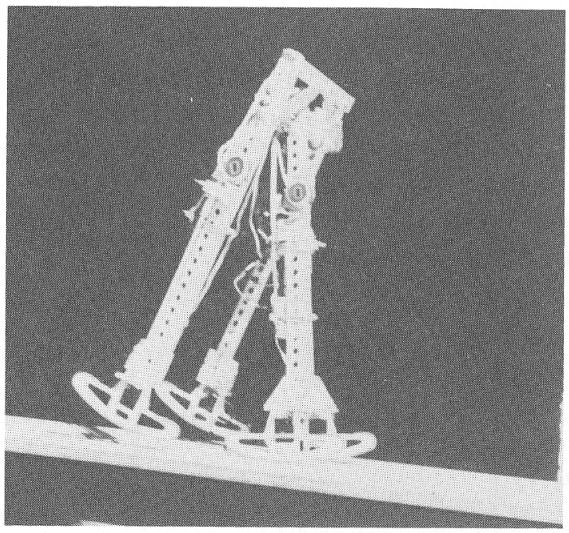

Figure 8: Our original straight-legged biped walking passively down a 2.5% slope. Weight is 3.5 kg and leg length 50 cm. Notice that the outer legs are paired like crutches to prevent lateral tipping. A leadscrew mechanism on each leg folds the swing feet sideways for clearance at midstride.

and can keep walking indefinitely.

To explore the feasibility of such cycles we formulate a *stride function* $\vec{S}$, which will map initial conditions $\vec{\nu}$ from one stride to the next:

$$\vec{\nu}_{k+1} = \vec{S}(\vec{\nu}_k) \tag{1}$$

$\vec{S}$ can be formulated analytically using linearised equations of motion, and in past work we have taken this approach [3]. However linearisation causes some noticeable loss in accuracy for gaits of normal speed, so alternatively $\vec{S}$ can be cast as a subroutine incorporating integration of fully nonlinear dynamical equations, recognition of end-of-step contact, and calculation of speed changes due to the impulse at heel strike. Whatever the formulation, however, a cyclic gait is indicated by an argument $\vec{\nu}_0$ which maps onto itself:

$$\vec{\nu}_0 = \vec{S}(\vec{\nu}_0) \tag{2}$$

This is a set of three equations which in general cannot be solved analytically, so we resort to Newton's method. Thus we differentiate the stride function (numerically) and linearise according to

$$\vec{S}(\vec{\nu} + \Delta\vec{\nu}) \approx \vec{S}(\vec{\nu}) + \nabla\vec{S}\ \Delta\vec{\nu} \tag{3}$$

Following Newton's method an initial estimate $\vec{\nu}$ for $\vec{\nu}_0$ can be improved by iteration of

$$\Delta\vec{\nu} = \left[\mathbf{I} - \nabla\vec{S}(\vec{\nu})\right]\left(\vec{S}(\vec{\nu}) - \vec{\nu}\right) \tag{4}$$

where $\mathbf{I}$ is the identity matrix. The result of this procedure depends upon the model parameters and the initial estimate. If the parameters are such that no cyclic gait exists

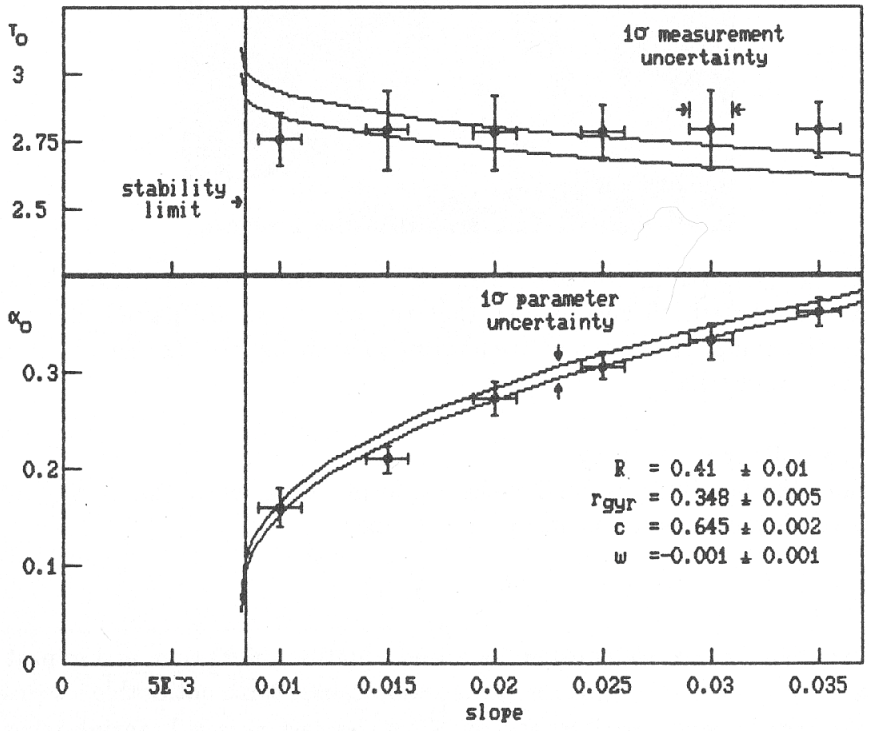

Figure 9: Analytical and experimental results for our first straight-legged biped. One time unit is 0.226 sec. Two sets of cyclic gaits can be calculated for this machine, but only the longer-period gaits could be observed quantitatively. The others were unstable. Each experimental point represents a composite of five trials on a 4 m ramp. Disagreements between the calculations and measurements are due in part to basing calculations on linearised equations of motion, and possibly in part to slightly elastic support transfer.

(*e.g.* on an uphill slope) or if the initial estimate is poor, then the iteration will quickly blow up. Otherwise, however, it will converge to one of *two* distinct solutions: that is, a model such as our experimental machine is in fact capable of *two* distinct passive gaits. Figure 9 shows the features of these gaits calculated over a range of slopes. It also shows the experimentally-measured features, which correspond to only one of the gaits. We have failed to observe the other, except over occasional fleeting steps, because it is unstable. The instability can be demonstrated using the linearised stride function. Suppose that at the start of step k the state vector is perturbed from $\vec{\nu}_0$ by $\Delta\vec{\nu}_k$. Then at the start of the next step $\Delta\vec{\nu}_{k+1}$ satisfies, according to (1) and (3),

$$\vec{\nu}_0 + \Delta\vec{\nu}_{k+1} \approx \vec{S}(\vec{\nu}_0) + \nabla\vec{S}\,\Delta\vec{\nu}_k \tag{5}$$

Cancelling the cyclic terms (2) leaves

$$\Delta\vec{\nu}_{k+1} \approx \nabla\vec{S}\,\Delta\vec{\nu}_k \tag{6}$$

This is just a set of three linear difference equations. Therefore transients following small perturbations can be analysed into three modes of the form

$$\Delta\vec{\nu}_k \sim \vec{\nu}_z\, z^k \tag{7}$$

where z is an eigenvalue of $\nabla\vec{S}$, and $\vec{\nu}_z$ is the associated eigenvector. For stability all three eigenvalues must have magnitude less than unity, with smaller magnitudes indicating that fewer strides are required to recover from a disturbance.

Table 1 lists the eigenvalues and eigenvectors calculated for the experimental machine walking on a 2.5% slope. We have given the modes names which roughly indicate their physical role: the "speed" mode is the principal means for eliminating perturbations in forward speed (reflected by its large amplitudes in Ω_C and α); the "swing" mode is the principal means for eliminating perturbations in Ω_F; and the "totter" mode is the principal means for responding to a mismatch between forward speed and step length (which normally satisfy $\alpha_0 \approx \Omega_{C_0}\tau_0/2$). More detailed discussion of them modes is offered in [3]. In the longer-period gait all three modes of the machine are stable, but in the shorter-period gait its totter mode is strongly unstable and quickly leads to toppling. With different parameter sets this problem can be tamed somewhat, but we have not found any cases in which the short-period gait is positively stable. In the long-period gait stability is much more reliable, being the rule over wide parameter variations, and holding for perturbations of useful (not merely infinitesimal) magnitude. Thus for example in experimental work we can start the machine manually, and rely on its own dynamics to handle imperfections in our technique.

2 Passive walking with knees

Our first machine left us with a lingering sense that the straight leg was not sufficiently realistic, and so in time we launched into a study of knees. We imagined a roughly anthropormorphic model, with the knee hinged freely in flexure but blocked mechanically against hyperextention. We formulated its stride function for motions of the general form shown in figure 3, with four initial conditions (one angle plus three rotational speeds), a

Table 1: Modes of the straight-legged machine on a 2.5% slope

	long-period gait			short-period gait		
mode	speed	swing	totter	speed	swing	totter
eigenvalue, z	0.692	-0.050	-0.825	0.591	0.076	9.606
α	0.653	0.136	0.993	0.391	0.191	0.643
Ω_C	0.736	0.149	0.113	0.638	0.385	0.592
Ω_F	0.179	0.979	-0.046	0.663	0.903	0.485

knee-free swing phase, an impulsive knee lock, a knee-locked swing phase, and an impulsive heel strike. We then set about searching for cycles following Newton's method. Our exploration was undertaken with fair optimism, since an earlier study of *ballistic walking* by Mochon & McMahon [9] had shown that passive dynamics could get a knee-jointed model through at least part of a walking cycle. Fortunately the promise of this work was soon borne out by our new stride function. Paired cyclic solutions emerged over a wide range of parameter variations, as in the straight-legged model. Anthropomorphic parameters proved to be particularly good, with a nicely stable long-period gait, comfortable ground clearance for the swing foot, and a positive locking torque on the stance knee maintained naturally throughout the stride. Thus the active mechanism used to clear the swing feet of our first biped now could be eliminated.

A selection of analytical results for these cycles is given in [5]. Here we add experimental data obtained with a machine called *Dynamite*. Figure 10 shows the machine, and figure 11 the calculated and measured walking behaviour. The agreement is better than in our straight-legged analysis because here the stride function was formulated using fully nonlinear dynamics. However while the solution for steady walking apparently is correct, experience suggests that the stability calculation is conservative. *Dynamite* regularly was able to walk the full length of our test ramp ($\approx$ 5 m) despite a calculated totter-mode eigenvalue of -1.5. Since both the steady-gait and stability analyses rely upon the same stride function, it is odd that there should be agreement on one and not the other; this discrepancy remains unresolved.

In the experimental work we also tested *Dynamite* with knees locked, thus reverting to the straight-legged model, and revisiting the problem of swing foot clearance. The solution for these trials was to put the machine on a chequerboard pattern of tiles. As the figure indicates gait timing and step length then proved to be quite close to those with knees-free, so the straight-legged dynamics continued to operate beneath all the new features.

Of course several important lessons had to be learned to obtain these results, and the main points to be made are as follows.

1. *Debouncing.* As the knee reextends during the latter part of the step, it makes hard contact with a mechanical stop. Once brought to rest against the stop it will stay there passively, but if it bounces it may still be flexed when the leg hits the ground. The result is usually catastrophic. To prevent bouncing and its unpleasant consequences we first tried hydraulic dampers under the kneecaps, but these proved

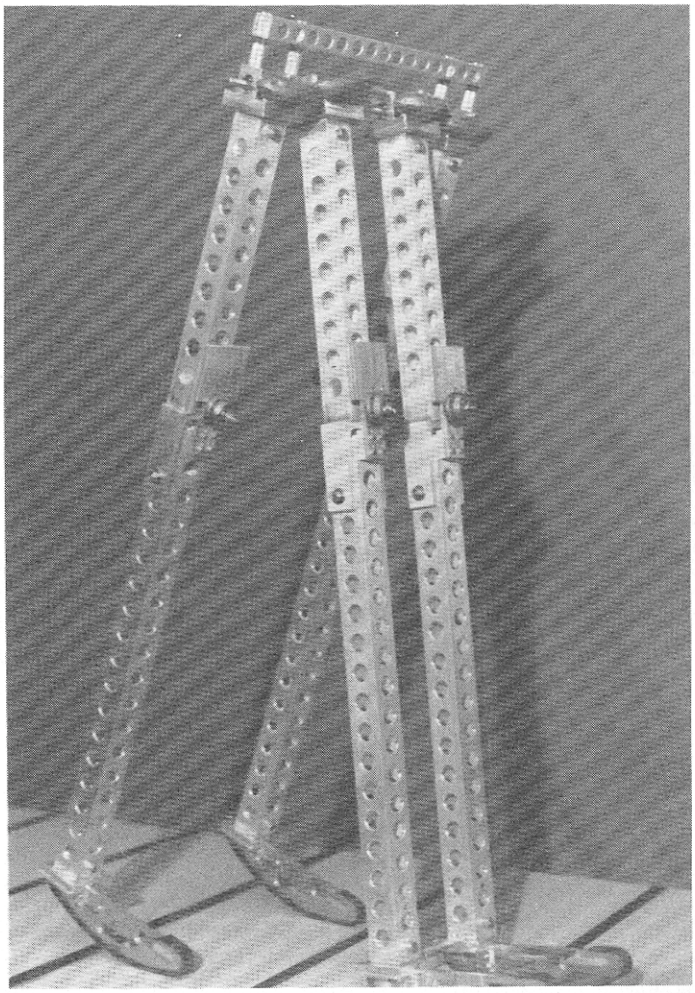

Figure 10: *Dynamite*, a two-dimensional biped with knees. Leg length is 80 cm, and mass 6.2 kg. Note the fishing weights on the hips, and on the shanks above the knees. The shank weights are attached to paddles which in this view hide the suction-cup knee debouncers.

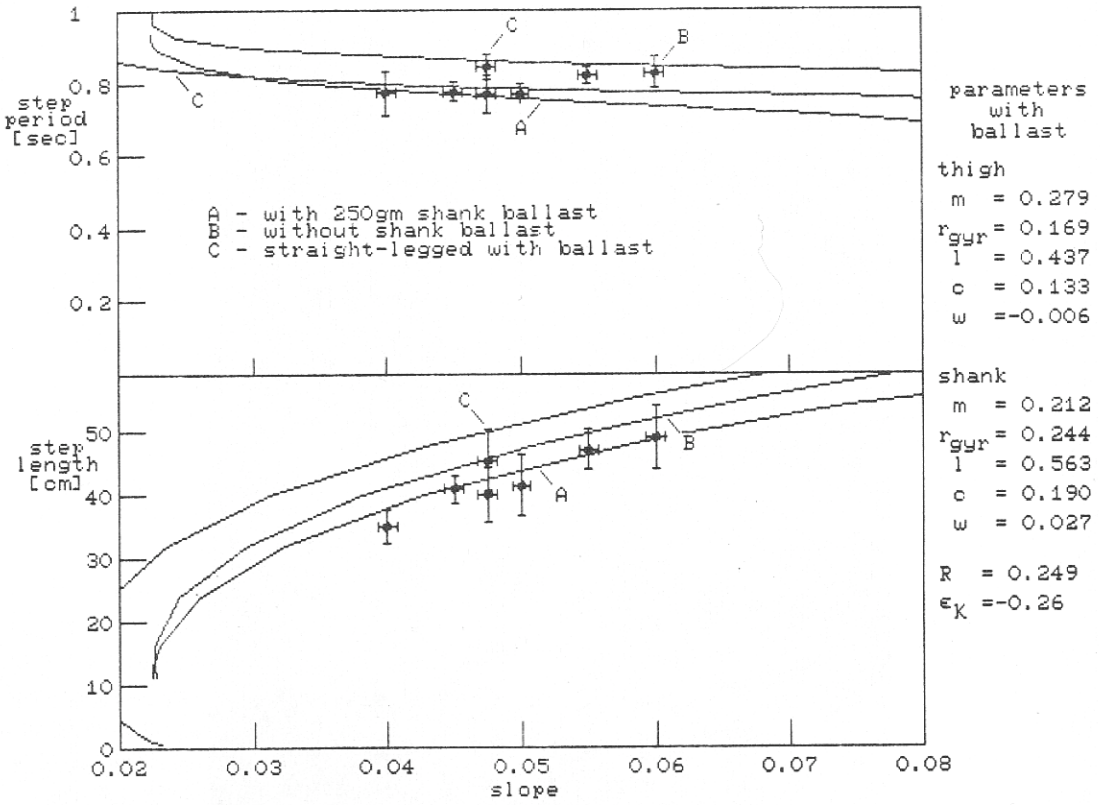

Figure 11: Walking behaviour of *Dynamite*. For the trials on 5% and shallower slopes the shanks were ballasted for improved foot clearance, as described in the text. On steeper slopes the ballast was eliminated. Each knees-free data point represents a composite of five trials, each of which included about a dozen steps. Fewer data were obtained in the straight-legged experiments. Difficulties arose because the machine had to be kept on a chequerboard pattern of elevated tiles for foot clearance, and moreover the straight-legged totter mode was calculated to be unstable. Nevertheless over many attempts we did manage a couple of straight-legged walks from start to end of the test ramp.

ineffective. Next we installed momentary mechanical catches, but these were tempermental and so not satisfactory. Finally we adopted a leaky suction cup, which proved very effective once we hit upon the right size for the leak. Sizing, however, remains tricky: the leak must be sufficiently slow to prevent ventilation of the cup during the few milliseconds of rebound, but at the same time must be sufficiently fast to prevent the cup from "grabbing" the shank when it is jerked into flexure by the impact of heel strike.

2. *Ballasting.* Impulsive energy losses, and hence the slope required for steady walking, are reduced by raising the overall mass centre of the model. *Dynamite* therefore had about 1 kg of lead across the hips. Furthermore for experiments on shallower slopes we also added 125 gm to the top of each half shank; the added inertia carried the swing leg into deeper flexure following support transfer, and so increased foot clearance. In general ballasting scales with the skeletal weight, and often carries an appreciable multiplier, so one must be careful to keep the basic structure light. *Dynamite* grew a bit out-of-hand in this respect, and so when it fell it was something of a hazard. A later machine, *Dynamite Jr.*, was smaller and caused its investigators much less apprehension on this account.

3. *Foot placement.* Whereas on the original straight-legged biped the feet were symmetric about the leg axis, on *Dynamite* they were displaced forward according to the anthropomorphic model. The reason was not just aesthetic. Forward displacement is required to put the contact force vector forward of the stance knee, and so keep it locked against its stop. Anthropomorphic sizing of the feet is also preferable, since much larger feet would reduce swing foot clearance, while much smaller feet would both increase dissipation at heel strike [3] and fail to provide locking torque unless the stance knee were allowed to hyperextend. Foot curvature is less important, but our semicircular shape is convenenient mathematically.

4. *Shank and thigh proportions.* A more subtle point of anthropomorphic design arose after our first iteration on *Dynamite* design. After a variety of computations had demonstrated that the knee-jointed model was reasonably robust we designed the experimetal machine. When assembly was complete we measured its mass distribution, and then set about calculating adjustments to be made by ballasting. The calculations revealed that no reasonable amount of ballasting would produce a satisfactory gait, that is, with stable eigenvalues, adequate foot clearance, and positive locking torque on the knee throughout the stance phase. We then systematically compared *Dynamite* with our successful anthropomorphic model, and discovered that the key difference was in the relative lengths of the shank and thigh. *Dynamite's* proportions were 50/50, but people have closer to 54/46; the shorter thigh turns out to generate substantially deeper knee flexion during the swing phase. We quickly modified *Dynamite* to 56/44, and immediately discovered a much broader range of ballasting options.

5. *Confidence in the analysis.* In responding to inquiries while preparing for experiments with *Dynamite*, we would reply quite honestly that if it didn't work we would be puzzled, but if it did work we would be amazed! When faced at the outset with

a machine whose only demonstrated abilities are very suddenly to topple face first or to buckle at the knee, analytical results often seem rather remote from the reality at hand. Under these circumstances persistence and flexibility are helpful, but one must above all maintain confidence that the analytical model is sound and that the mechanical implementation is faithful. We in particular had the problem of how to start the machine, which we tried to address through more than a month of unsuccessful tinkering with an automatic launcher. Ultimately we hit upon a manual starting technique that worked with passable reliability, and so obtained the results discussed above.

Of course once viewed in action the knee-jointed cycle, however surprising on paper, soon seems perfectly normal: seeing is believing. (Interested readers can obtain video for this purpose either from the IEEE [4] or directly from me.) Unfortunately, however, we still cannot claim good intuition about the physics of the cycle. Ballasting, for example, is guided by calculations and previous results rather than by a more holistic feeling for the dynamics. This remains a handicap, as better intuition would doubtless accelerate the evolution of improved walking models.

3 Three-dimensional walking

Let us now step out of the two-dimensional bounds of the preceding pages and consider how to operate in a three-dimensional world. As a first intermediate imagine a biped which is two-dimensional in design (that is, which has no lateral thickness and so can swing its legs past each other in the same plane) but nevertheless has freedom to move in three dimensions. Then its "three-dimensional" steady gait is the same as in 2D, and the only new complication is associated with stability – or more to the point, *instability*, since in the lateral plane the model behaves more or less as inverted pendulum. (One might hope for a "rolling coin" dynamic effect to stabilise the lateral motion. However the rolling coin owes all of its stability to spin, and a biped doesn't have the necessary store of angular momentum since its legs counter-oscillate.) Thus a small perturbation in yaw will quickly cause a steepening spiral turn followed by a sideways crash.

At this point we might observe that the 2D model also has inverted-pendulum features in the longitudinal plane, but manages to stabilise itself by periodically exchanging support between legs set some distance apart. Following this observation we might expect out-of-plane stability to benefit from lateral leg separation. Lateral separation, however, raises the question of whether and how a passive model might counter the unsupported weight of the swing leg. One can certainly attempt to reason out a scheme, but for those whose 3D intuition is unreliable there is also the option of blind recourse to numerical methods. We conceded membership in the latter category and so developed a new stride function for the 3D model sketched in figure 12. This model has *seven* start-of-step variables: yaw, roll, and stance pitch angles (swing pitch is determined by the contact condition) plus rates about the three stance leg axes, plus interleg pitch rate about the hip. The motion is calculated using fully nonlinear dynamics (which for security we derived once by hand and again using the *Autolev* program [10]). End-of-step conditions are conservation of the angular momentum vector $\vec{H}$ of the whole machine about the point of heel strike, and of $\vec{H} \cdot \hat{z}_c$ about the hip. These determine the change in rotation rates at

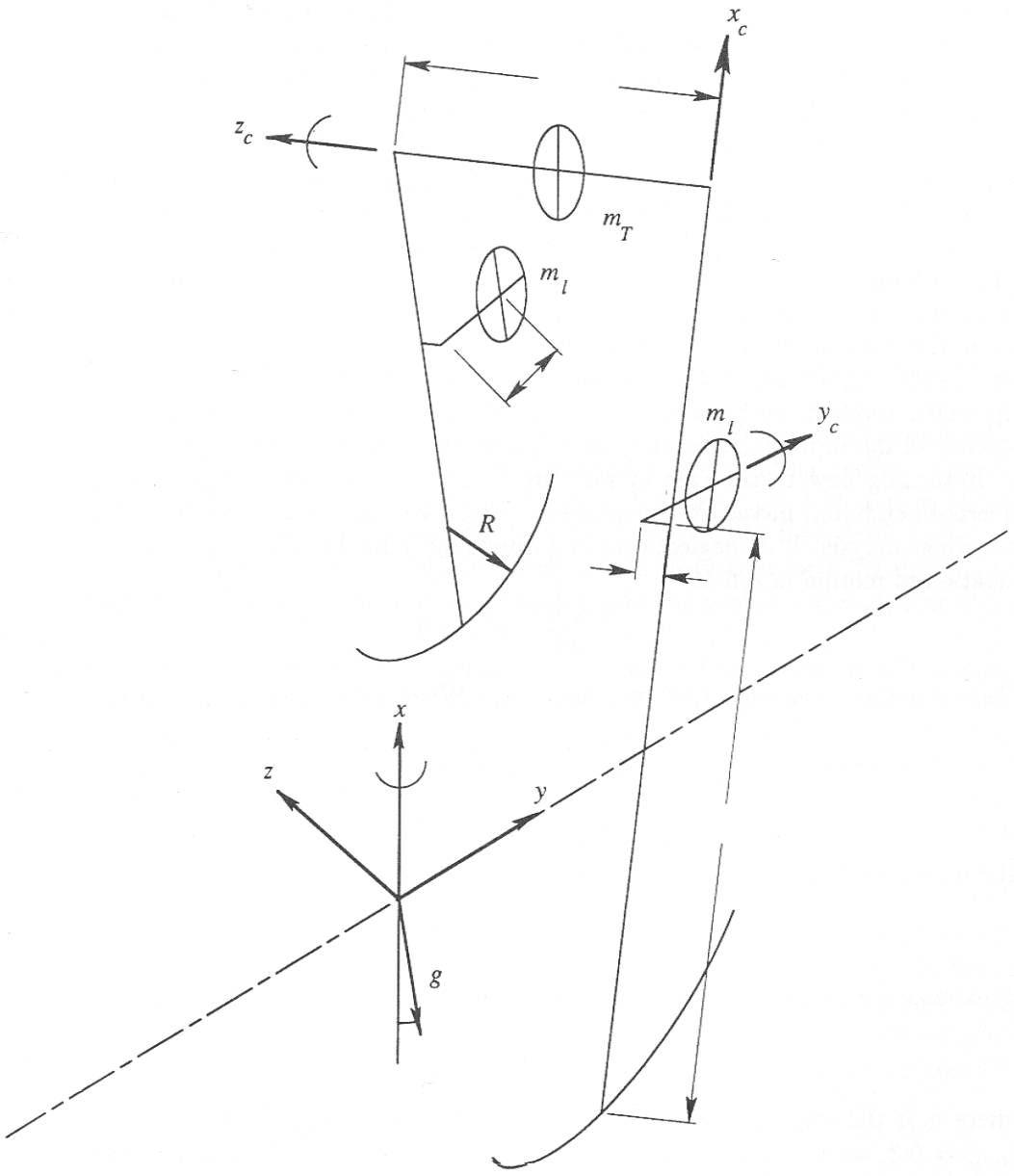

Figure 12: A three-dimensional passive biped. Like the original 2D model it has straight legs and semicircular feet. Orientation of the stance leg relative to the ground coordinates is determined by the yaw (ψ), roll (ϕ), pitch (θ) sequence of rotations about the axes indicated. The swing and stance legs have the same yaw and roll angles, but can pitch independently. Mass centres are shown for the legs and hip; those on the legs have 3D rotational inertia, while the hip axle carries only a point mass.

impact, and so together with the equations of motion complete the stride function. Once this was encoded in FORTRAN we applied the cycle-searching procedure (4), looking first at models with narrow hips as for them the 2D solution provided a good estimate to start the iteration. Note that in 3D the search must look not for initial conditions which repeat, but rather which produce a mirror image on the succeeding step. Yaw and roll therefore should change sign from one step to the next.

Thankfully the search procedure did turn up cyclic solutions, as plotted for example in figures 5 and 13. Let us begin with figure 13, which shows the effect of hip width on gait. As the hips widens, both the short- and long-period passive gaits evolve from their distinct 2D forms, until they merge at a hip width of about $0.42l$. Passive walking cannot be sustained with wider leg spacing, unless some adjustment is made in the other parameters of the model. One parameter which can be used to good effect in this direction is Δy, the fore/aft offset in the leg's mass centre. Notice that in this example we put the mass centre slightly aft of the leg axis. Had we instead put it on the axis, the acceptable hip width would have been substantially reduced. This is but one illustration of the potency of Δy in modulating gait; other examples are discussed in [3] and [1].

Returning now to the case of zero hip width, notice that each gait has the strong inverted-pendulum instability mentioned earlier. We can explain the magnitude by the following analysis. If we neglect coupling from longitudinal motion, then we can write the equation of motion in roll as

$$\frac{d^2\phi}{dt^2} - \sigma^2\phi \approx 0 \tag{8}$$

where σ is the (inverted) pendulum frequency. When normalised by $\sqrt{g/l}$ this is

$$\sigma = \sqrt{\frac{2m_{leg}c + m_T}{2m_{leg}(c^2 + r_{gyr_y}^2) + m_T}} \tag{9}$$

The dominant term in the rolling solution is then

$$\phi \sim \phi(0)e^{\sigma\tau} \tag{10}$$

By comparison with (7) we therefore should expect a mode with

$$z \approx e^{\sigma\tau_0} \tag{11}$$

where τ_0 is the step period. In the example of figure 13, $m_{leg} = 0.4$, $m_T = 0.2$, $c = 0.6$, $r_{gyr_y} = 0.3$, so σ is 1.10, and z then works out to 9.96 for the short-period gait and 20.1 for the long-period. By comparison the values calculated using (7) are about 16 and 24, respectively; the aggravated instability in the full model apparently arises from an "anti-rolling-coin" effect due to the angular momentum of the swing leg.

As anticipated this spiral instability moderates if some lateral separation is put between the legs. Unfortunately that is not to say that the instability disappears. Instead as w_{hip} increases not only does the spiral mode ultimately "bottom out" with $|z| \approx 5$, but several other modes go unstable as well. Table 2 lists these bad actors for the long-period gait with $w_{hip} = 0.15$. Furthermore explorations through parameter space have failed to turn up any set of parameters with which the situation is much better. Therefore some

Table 2: Unstable modes of example long-period gait with $w_{hip} = 0.15$

mode	spiral			directional
eigenvalue, z	-10.340	4.341	2.224	-1.066
θ_C	-0.319	0.547	0.471	-0.009
ϕ	0.592	0.166	-0.056	0.032
ψ	0.074	-0.688	-0.364	-0.999
ω_x	0.380	0.145	-0.176	-0.010
ω_y	0.608	0.223	-0.179	0.002
Ω_C	0.061	0.136	0.675	0.008
Ω_F	-0.157	0.333	0.351	0.010

variation on the model appears to be necessary for stabilisation of 3D passive walking, and we will suggest measures below.

However let us not be too hasty to dismiss the present model, for the character of its steady cycles is well worth examining. Notice first that the longitudinal motion is hardly different from that in the 2D cyclic gait (*cf.* figures 5, 2) save for the fact that in 3D the motion is somewhat accelerated. Hence the lessons of the straight-legged 2D model can be applied in the 3D case. Presumably the same would prove true for a 3D model with knees, which in particular we would expect to eliminate the problem of midstride swing clearance.

Moving on to the uniquely 3D behaviour, notice that the amplitude in roll is nearly nil while that in yaw is quite large. This combination is surprising in view of the exactly opposite strategy of our introductory toy. Its cycle develops pronounced roll but little yaw; in fact a quadrupedal cousin of the toy cannot yaw at all. The differences between the models can be ascribed to foot design. In the sagittal plane the toy's feet form a circular section centred *above* the overall mass centre. Lateral rocking then reduces to a lightly-damped pendulum oscillation, and to make the toy work well the body-rock and leg-pitch pendulums should be tuned with frequencies roughly in the ratio 3:4 [3]. The model of figure 12, on the other hand, has blade feet and so cannot rock without dissipating a lot of energy. It therefore eliminates rocking, and instead arranges for lateral balance by exploiting centrifugal effect in a turn. The balance can be demonstrated as follows. The centrifugal acceleration of each mass centre is $V\dot{\psi}$, V being the local speed tangent to the turn and $\dot{\psi}$ the yaw rate. The net centrifugal torque, when normalised by mgl, is therefore roughly

$$V\dot{\psi}\,(2m_{leg}c + m_T) \approx \frac{2\alpha_0}{\tau_0}\frac{2\Delta\psi}{\tau_0}\,(2m_{leg}c + m_T) \tag{12}$$

where α_0 is the excursion of the stance leg in pitch, and $\Delta\psi$ the excursion in yaw. (Note that the local speed is less than $2\alpha_0/\tau_0$ at the stance mass centre, but greater at the swing mass centre; the differences cancel.) Meanwhile the centripetal torque due to the unsupported weight of the hip and stance leg is approximately

$$m_{leg}w_{hip} + m_T\frac{w_{hip}}{2} \;=\; \left(m_{leg} + \frac{m_T}{2}\right)w_{hip}$$

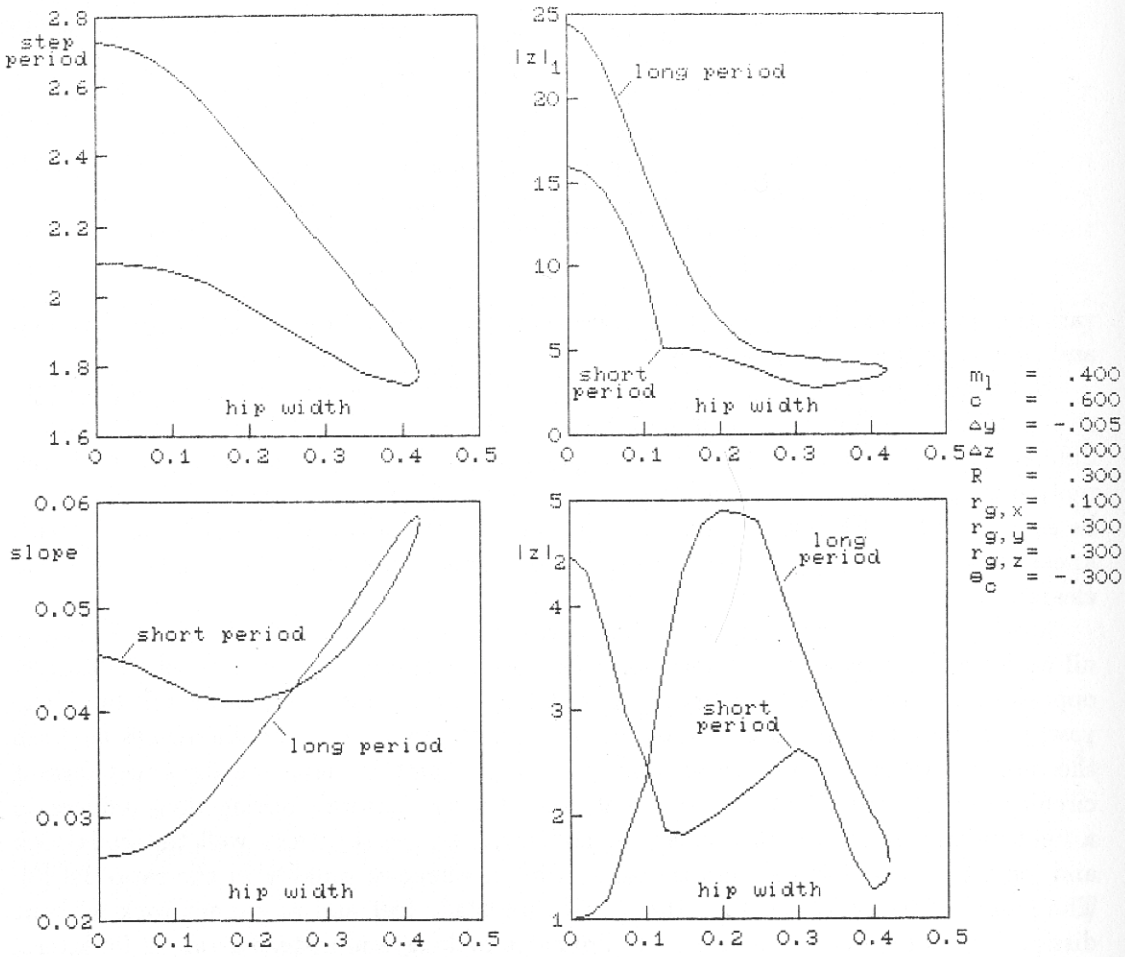

Figure 13: Step periods, equilibrium slopes, and dominant eigenvalues calculated for 3D passive bipeds walking with a stride of about 0.6 leg length (initial $\theta_C = -0.3$). Results for both short- and long-period cycles are plotted against hip width. Evidently passive walking can be maintained even with quite wide hips, although at some cost in dissipation at heel strike (hence the steepening slope). As the width increases the spiral instability is substantially moderated, but other modes go unstable, and the cyclic gaits "pinch off" before absolute stability is achieved. Parameters of the model are listed in the margin.

$$= \frac{w_{hip}}{2} \tag{13}$$

Balancing torques implies that

$$\Delta\psi \approx \frac{w_{hip}}{2} \frac{\tau_0^2}{4\alpha_0} \frac{1}{2m_{leg}c + m_T} \tag{14}$$

In the example of figure 5 this formula suggests $\Delta\psi = 0.58$, which agrees fairly well with the amplitude of 0.64 actually calculated for the cyclic gait.

It is interesting to ask how the model manages to sustain such a large yawing motion. To see the mechanism one should imagine the geometry just at the start-of-step, with the swing leg well behind the stance leg. Its unsupported weight then applies a modest rolling moment to the stance leg, but also a quite substantial yawing moment. The latter moment starts the model turning towards its centreline. The yawing torque drops to zero at midstride, and then builds in the opposite direction so that the turn straightens up by the end-of-step.

Relative to the toy our model has three apparent advantages: first, it is less tippy in roll, *i.e.* given a modest jolt with both feet on the ground, it will damp rocking cycles more quickly. Second, its feet have simpler geometry. Third, it is more robust with respect to parameter variations, because there is no requirement for tuning pitch and roll frequencies. However the model still has unsatisfactory characteristics. The yawing motion is much too exaggerated by anthropomorphic standards, and leads to excessive lateral motion of the hip. Furthermore the instabilities in the gait must somehow be controlled.

Inspection of the human model suggests how the situation can be improved. The most significant point is that we have three-degree-of-freedom hips. The rolling degree of freedom seems particularly useful, as one can quickly surmise by attempting to walk with the same constraints as our model. That is, try walking while keeping the legs as far apart at the feet as at the hips – it will feel awkward! Compare this with walking on a balance beam, with footfalls almost collinear – much easier! Evidently we use the roll freedom to reduce lateral separation between the legs, and so eliminate most of the rolling torque. Moreover the ability to modulate lateral leg separation provides a powerful control, not only for stabilisation but also for steering [12].

Hence the next recourse for the 3D model becomes evident: install roll joints at the top of each leg. These cannot be left freely hinged like the pitch joints, since if they were then the hip axle would collapse as soon as the swing leg were left unsupported. Instead stiff torsional springs must be included. We are reasonably confident that a model with joints thus stiffened will have passive gaits, but we are less sanguine about stability: it will have four modes in addition to the present model's seven, and only a committed optimist would imagine all eleven eigenvalues clustered within the unit circle! However one could stabilise the cycle by varying the equilibrium positions of the roll springs; in the next section we will outline how to develop a control law.

4 Pumped passive walking

All of the models considered thus far have been analysed under gravity power. This formulation is attractive in that it lets the models do entirely as they like, so to speak,

unencumbered by any muddling of control with dynamics. However if we look carefully at how the models do as they like, we can also discover how they could do more of what we want – in particular, how they could walk uphill.

As an aid to looking carefully, imagine a reversible projector running film of a straight-legged biped (in either 2D or 3D). Run the projector in one direction, and you see the model going downhill. Run in the other, and you see it going uphill. But which direction is forward in time? You cannot say! On the one hand, you might be looking at a biped strolling downhill, dissipating energy in an impulse at each heel strike. But on the other hand, you might be looking at a biped pumping uphill, supplying energy by an impulse at each toe-off. Both interpretations are fully consistent with the equations of motion.

Of course one might protest that this sounds like a lot of smoke-and-mirrors: the biped with supposed upward mobility couldn't generate those impulses in practice, and anyway this trick wouldn't work on a knee-jointed model, which after all is the most realistic of the lot. These objections would be entirely correct. However, they also would be rather beside the point. With respect to the knee-jointed model, figure 11 indicated that its dynamics are not so unique as they first might appear. And with respect to impulses, indeed they are artificial; however, they also offer a good first approximation to what could be implemented by a machine, and to what actually is implemented (via *dorsiplantarflexion*) by people.

Thus we immediately have a solution for walking uphill: all we need do is calculate the heel-strike impulse in downhill walking, and apply the mirror image. But we are still left with the most basic problem of all: how to walk on the level? The "projector argument" suggests that the solution should be symmetric, with energy input by an impulse at toe-off and dissipated by a mirror-image impulse at heel strike. But we still don't know what impulses will work. Thus we are left again appealling to a cycle hunt via the stride function. In this case the formulation must include impulse-coupling terms as well as the heel-strike conditions and swing dynamics. With this in hand (as derived in [1]) the protocol is simply to specify an impulse (by magnitude and direction) and then apply (4) to find a cyclic gait. The results prove to be quite consisent with those for passive models, but still perhaps a bit surprising at first glance.

First, for any specified impulse, cyclic gaits come in pairs, as in the gravity-powered model, but only one of the two gaits is symmetric. Second, such pairs can be generated by a wide range of impulse choices. Figure 14 illustrates these points in the form of a contour plot (for a 2D model) on axes of impulse energy and direction. For any point in this space a pair of gaits can be calculated, although in some areas (show as broken contours) one or the other is formally inadmissable because the impulse would throw the model off the ground. (Mathematically the heel strike impulse then becomes a non-physical downward pull.) The asymmetric gait in the pair turns out to have a cadence exactly twice the frequency of the leg swinging as a free pendulum. Meanwhile the symmetric gait may have a higher or lower cadence depending upon how the impulse is applied.

Figure 14 is good news for engineers aspiring to biped de ign, since its essential message is that anything goes: *any* reasonable choice of impulse will generate at least one gait and quite possibly two. Which (if either) of the two gaits develops depends upon how the biped starts, and upon stability, although with the possibility of varying impulses from one step to the next we could actively stabilise one gait and prevent development of another. We will discuss algorithms after making some further observations on the dynamics of steady

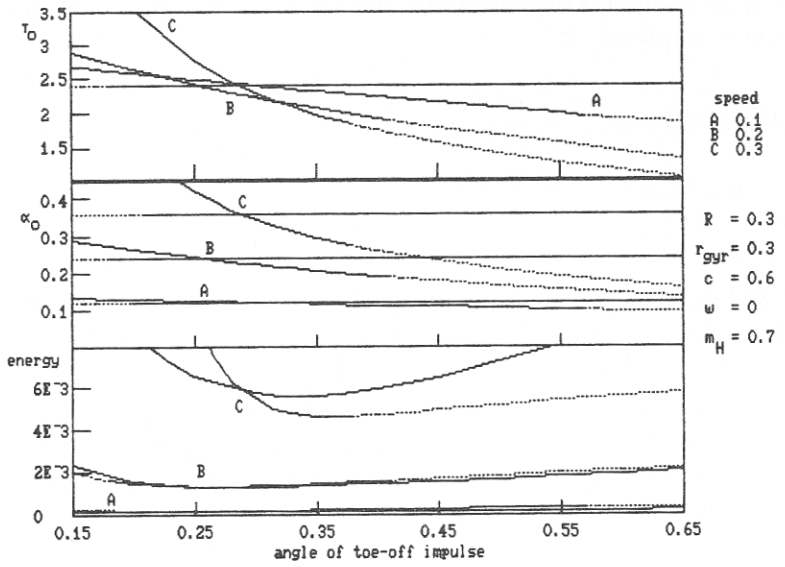

Figure 14: The energy necessary to sustain a walking cycle on level ground can be supplied by a toe-off impulse on the trailing leg. Here the bottom plot shows contours of constant walking speed as a function of impulse energy (normalised by mgl) and angle (forward from the vertical). The top plot shows the corresponding step period, and the middle plot the start-of-step leg angle. It turns out that there are two sets of solutions for each walking speed, and hence two contours.

walking.

Our earlier "projector argument" revealed one impulse for climbing uphill, but none for walking on level ground. Now having seen that there is in fact a multitude of impulses that will work for level walking, we should investigate whether the projector also failed to tell the full story for climbing. Indeed stride-function calculations reveal much more; impulses over a range of angles and energies will generate a cyclic climb. (Details are given in [6] and [1].) However it turns out that the admissable region of impulse space shrinks considerably as the slope increases, so that impulses alone ultimately are restricted only to rather shallow slopes.

For steeper slopes two options are available. The first is to vary leg length cyclically, making the leg on the uphill side short and the downhill side long. A good approximation for the necessary amplitude is

$$\begin{aligned} mg\ 2\alpha_0\ l\ (\gamma_g - \gamma) &\approx mg\ 2\Delta l \\ \text{energy required} & \quad \text{energy input} \\ \text{for climbing} & \\ \Rightarrow \frac{\Delta l}{l} &\approx \alpha_0\ (\gamma_g - \gamma) \end{aligned} \tag{15}$$

where γ_g is the slope required for walking with no length variation. With this as the pumping mechanism (or braking mechanism when travelling downhill) cyclic gaits can be sustained on slopes as steep as a normal staircase [1].

A second method is to grow a torso and lean it in the appropriate direction. Thus for descent the torso would be held in a backward recline by reaction against the stance leg; the effect is to brake the stance leg at the hip. The braking torque with the torso at angle β from the vertical is

$$T_H = -m_T g c_T \sin\beta \tag{16}$$

where the torso has mass m_T centred a distance c_T from the hip. The energy dissipated through one step is then

$$W = -\int_{-\alpha_0}^{\alpha_0} T_H d\theta_C = 2m_T g c_T \sin\beta\ \alpha_0 \tag{17}$$

Meanwhile the excess energy gained in descending slope γ is

$$E = 2mgl\alpha_0(\gamma - \gamma_g) \tag{18}$$

so that the required torso recline is

$$\beta = \sin^{-1}\left(\frac{-m}{m_T}\frac{l}{c_T}(\gamma - \gamma_g)\right) \tag{19}$$

Cycle analysis for the 2D biped with torso shows that such a model can maintain stable descents on moderately steep slopes [1]. Climbing then follows by the projector method: a film of a descending biped with a backward inclination, dissipating energy via impulses and braking, could just as easily show a climbing biped with a forward bent, thrusting itself upward via impulses and hip exercise. Again both interpretations are dynamically admissable.

However a problem with relying on the torso to facilitate climbs and descents is that it isn't very powerful; with anthropomorphic values of $m_T = 0.7$ and $c_T = 0.3$, (19) dictates that the torso lean seven degrees for each degree of slope. Hence on even moderately steep slopes it runs out of leverage, and the model must revert to leg-cycling. A second problem is that the the torso is essentially an inverted pendulum, so that the torso/stance leg torque has to be adjusted actively to keep it near the desired angle. Thus for example in figure 4 the stance/torso torque is specified by a proportional-derivative feedback law on torso angle. It is interesting that human evolution has accepted this control task rather than arrange for the torso to be statically stable, as might perhaps be accomplished by moving the hips up to the shoulders. One reason might be that when standing still there would remain a control problem due to the static instability of the legs; solving that takes care of the torso as well.

5 Stability augmentation and gait modulation

Let us now take up the question of how to actively stabilise a passive gait, and how to modulate it from step to step. For a first example we shall suppose that the control is torque T_H between the legs (applied in practice by adding T_H to the stabilising torque between the stance leg and torso, and offsetting it by $-T_H$ between the swing leg and torso). We will allow T_H to change between steps, but will hold it constant through any one step. To estimate its effect we use the stride function. Thus from (5)

$$\vec{S}(\vec{\nu}_0 + \Delta\vec{\nu}_{k+1}, T_H) \;\approx\; \vec{S}(\vec{\nu}_0, T_H = 0) + \nabla\vec{S}\;\Delta\vec{\nu}_k + \nabla_T\vec{S}\;T_{Hk} \tag{20}$$

Cancelling cyclic terms as in (2) leaves

$$\Delta\vec{\nu}_{k+1} \;\approx\; \nabla\vec{S}\;\Delta\vec{\nu}_k + \nabla_T\vec{S}\;T_{Hk} \tag{21}$$

Here we have a set of linear difference equations in standard form, which invites a standard linear control law:

$$T_{Hk} = \mathbf{C}\,(\vec{\nu}_0 - \vec{\nu}_k) \tag{22}$$

Familiar methods of controller design (*e.g.* LQR) can now be brought to bear. (Formal controllability is unlikely ever to be a problem.) [2] gives an example of this procedure applied to active stabilisation of running. Notice that to implement the controller one need sample the state of the model only once per stride.

While mathematical methods of controller design thus come readily to hand, one can also imagine a physical approach motivated by what might be called the "stepping stone" problem. Here the objective is to precisely modulate footfalls from one step to the next, which implies that α_{k+1} is specified for all k. According to (21), the hip torque required to achieve the desired step length is

$$T_{Hk} = \frac{1}{\nabla_{T,1}\vec{S}}\left(\Delta\alpha_{k+1} - \nabla_1\vec{S}\;\Delta\vec{\nu}_k\right) \tag{23}$$

where $\nabla_{T,1}\vec{S}$ is the first element of $\nabla_T\vec{S}$, and $\nabla_1\vec{S}$ the first row of $\nabla\vec{S}$. Thus in this formulation

$$\mathbf{C} = \frac{1}{\nabla_{T,1}\vec{S}}\;\nabla_1\vec{S} \tag{24}$$

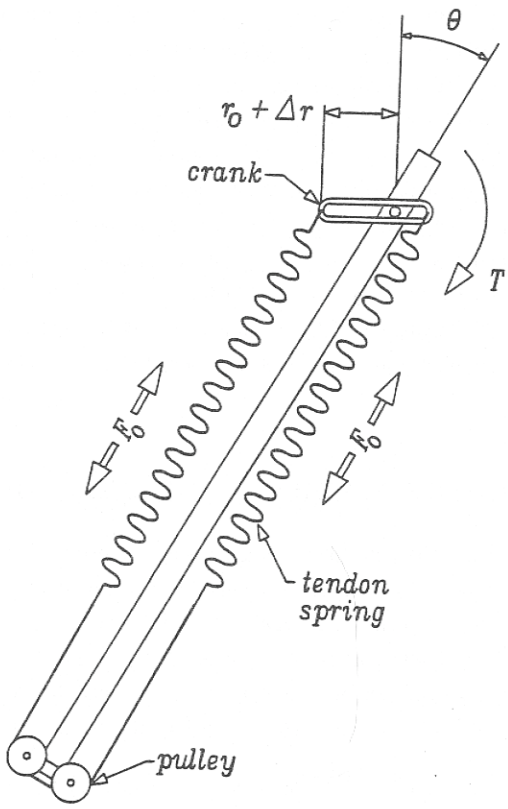

Figure 15: A hip actuator using Levered Isotonic Tendons for Human Emulation: LITHE. The pulleys maintain equal tensions in the two antagonistic tendons, while differential adjustment of their mechanical advantage determines the net torque about the crank. Elasticity in the tendons keeps the tension, and therefore the torque, constant over large swings in leg angle.

In many cases this choice is quite satisfactory. However in others it can lead to unstable modes in the remaining elements of $\vec{\nu}$. If one wants to do "stepping stone" control in these cases, one must invoke other controls – toe-off impulses, length cycling, and (in our proposed 3D development) roll-spring-equilibria – to take care of the stabilisation problem. Thus in general one could write (20) as

$$\Delta\vec{\nu}_{k+1} \approx \nabla\vec{S}\,\Delta\vec{\nu}_k + \nabla_c\vec{S}\,\vec{u} \tag{25}$$

where $\vec{u}$ includes all of the control variables. Following (23) some of these could be used to set elements of $\vec{\nu}_{k+1}$ directly (*e.g.* α_{k+1} for step length, ψ_{k+1} for steering). One would then be left with a system of reduced order, which could be stabilised using those variables not already "used up" for step-to-step modulation.

6 Powered walking experiments

Work on powered walking has been taken up by the Carnegie-Mellon Robotics Institute, and an experimental machine is nearing completion. It is a straight-legged 2D biped with a torso, having 1 m leg length and an anticipated mass of 20-30 kg. It will be impulse-powered by spring-loaded pistons acting between each leg and foot. These will be cocked by small motors during the stance phase, and then fired just before heel strike.

Hip actuator design has required particular care. At support transfer the stance/torso torque must be switched quickly across the hips; otherwise the suddenly unrestrained swing leg will get a big kick! The hip actuator therefore must be fast. Moreover, it must be supple: when acting on a dangling leg, it should set the equilibrium position, but not affect the pendulum frequency or damping. The geared motors or fluidic actuators used on most mechanical bipeds do not satisfy this requirement; lift one of their legs, and it will hang catatonically or, at best, grind slowly to a halt at the bottom of its swing. With joints like these the physics of passive walking are reduced to so much background noise. To preserve dynamics we have developed the so-called LITHE actuator shown in figure 15. The mechanism has proved to be quite satisfactory in balancing a leg inverted, and we look forward to equally good performance in walking experiments.

7 The collection of results

The models that we have outlined are together capable of a strong repertoire of locomotion, including walking at a range of speeds, in two or three dimensions, up and down slopes steep and shallow, and over unevenly-spaced footholds. All of this repertoire is built upon the robust foundation of the elementary passive cycle, which leads to efficient performance and simple control methods for the design engineer (and, one might imagine, a forgiving feel for a child finding his feet). In this light legs seem not so complicated after all.

At present, however, the elements that we have mentioned remain in pieces. Obviously the long-term objective is to bring them together, and the immediate opportunities for progress seem to be the following.

1. Completion of the 2D, powered, straight legged biped, and demonstration of climbs, descents, and stepping-stone control using impulse energy, torso inclination, and hip torque for pumping and modulation.

2. Design of a 2D powered biped with knees. If left without a torso this will be simpler than the current powered biped project, but more aesthetically pleasing because of the anthropomorphism. Initial analytical work is required to test impulsive pumping in the knee-jointed model (by plantarflexion), but this is likely to be successful in view of the robustness of the passive gait with respect to impulse angle and energy.

3. Analytical development of the proposed 3D model with roll springs at the hips. If this model proves to have cyclic gaits, then an experimental machine could be built (which, as mentioned earlier, would probably need active stabilisation according to the formulation of (25)). Alternatively the analytical work might be extended further by addition of knees.

Should the work on this agenda prove successful, the next step would be to make a steep-slope machine (probably with knees) pumped by leg-length cycling. That in turn would open a number of paths leading to a "full repertoire" biped, but further mapping is best left until the landscape is better known. Of course, there is also an agenda to be developed for passive *running*; figures 6 and 7 hardly begin to scratch the surface. That, however, is another story entirely.

References

[1] Tad McGeer. Dynamics and control of bipedal locomotion. 1991. Submitted to the Journal of Theoretical Biology.

[2] Tad McGeer. Passive bipedal running. *Proceedings of the Royal Society, Series B*, 1240(1297):107–134, 1990.

[3] Tad McGeer. Passive dynamic walking. *International Journal of Robotics Research*, 9(2):62–82, April 1990.

[4] Tad McGeer. Passive dynamic walking with knees. In *Video Proc. 1991 IEEE Robotics & Automation Conference*, Sacramento, California, April 1991.

[5] Tad McGeer. Passive walking with knees. In *Proc. 1990 IEEE Robotics & Automation Conference*, pages 1640–1645, Cincinnati, Ohio, May 1990.

[6] Tad McGeer. Principles of walking and running. In R. McNeill Alexander, editor, *Mechanics of Animal Locomotion*, Springer-Verlag, Berlin, 1991. (In press).

[7] Tad McGeer. *Stability and Control of Two-dimensional Biped Walking.* Technical Report CSS-IS TR 88-01, Simon Fraser University Centre for Systems Science, September 1988.

[8] Thomas A. McMahon. Mechanics of locomotion. *International Journal of Robotics Research*, 3(2):4–28, 1984.

[9] Simon Mochon and Thomas A. McMahon. Ballistic walking: an improved model. *Mathematical Biosciences*, 52:241–260, 1980.

[10] David B. Schaechter, David A. Levinson, and Thomas R. Kane. *Autolev 1.2.* OnLine Dynamics, Inc., 1605 Honfleur Drive, Sunnyvale, California, 1988.

[11] Clay Thompson and Marc Raibert. Passive dynamic running. In V. Hayward and O. Khatib, editors, *Int. Symp. of Experimental Robotics*, pages 74–83, Springer-Verlag, New York, 1989.

[12] Miles A. Townsend. Biped gait stabilisation via foot placement. *Journal of Biomechanics*, 18(1):21–38, 1985.